SLAC-PUB-7817
April 1998

Electron-hose instability in an annular plasma sheath

David H. Whittum
Stanford Linear Accelerator Center, Stanford University, Stanford California, 94309

Abstract

A relativistic electron beam propagating through an annular plasma sheath is subject to a transverse plasma-electron coupled electrostatic instability. From the linearized fluid equations, the beam-sheath interaction is resolved into three coupled equations. The corresponding wakefield is computed and the asymptotic linear evolution is noted. For illustration, numerical examples are given for a plasma accelerator employing such a sheath. While the coasting beam scalings are quite severe at low energy, single-bunch instability growth can in fact be reduced to nil, for a very high-gradient accelerator.

Paper submitted to J. Phys. D: Appl. Phys.

(Work supported by Department of Energy contract DE-AC03-76SF00515)

Electron-hose instability in an annular plasma sheath

David H. Whittum
Stanford Linear Accelerator Center
Stanford University, Stanford CA 94309

(Received)

A relativistic electron beam propagating through an annular plasma sheath is subject to a transverse plasma-electron coupled electrostatic instability. From the linearized fluid equations, the beam-sheath interaction is resolved into three coupled equations. The corresponding wakefield is computed and the asymptotic linear evolution is noted. For illustration, numerical examples are given for a plasma accelerator employing such a sheath. While the coasting beam scalings are quite severe at low energy, single-bunch instability growth can in fact be reduced to nil, for a very high-gradient accelerator.

PACS: 52.40 Mj, 29.25 Fb, 52.35 Py and 52.50 Gj.

I. INTRODUCTION

Much current work in accelerator and radiation research focuses on the propagation of intense electron beams through plasma. Stability against transverse beam break-up[1] is critical in such applications and is the subject of many works, treating resonant interaction with structure modes,[2] instability due to lossy walls,[3] image return current displacement due to gaps in the beamline[4] and beam-plasma interactions such as ion-hose[5] and resistive hose.[6] Until recently less attention has been given to the *transverse* two-stream instability[7,8] arising from the presence of a low energy electron population in the beamline.

Sources of such excess electrons in the beamline include beam ionization,[9] multipactor,[10] and laser-ionization. Applications such as ion-focused transport[11] and laser-wakefield acceleration[12] or plasma-wakefield acceleration[13] can all access a regime in which an annular plasma surrounds an electron beam as it propagates down the beam tube.

In this work, transverse beam break-up due to an idealized uniform density finite plasma sheath is considered for a cylindrical geometry. In Sec. II the transverse problem is formulated in terms of three coupled equations describing the beam-sheath interaction. In Sec. III the wakefield is computed, and in Sec. IV, instability growth is examined. In Sec. V, some conclusions are offered.

II. COUPLED BEAM-SHEATH EQUATIONS

The equilibrium configuration is depicted in Fig. 1, consisting of an annular plasma sheath with inner radius b_1, and outer radius b_2, contained within a perfectly conducting pipe of radius R. Return currents within the plasma are neglected in the limit of large plasma skin depth, and the plasma is assumed collisionless and initially uniform within the annulus. The beam is assumed to be uniform out to radius a, with prescribed linear focusing characterized by betatron wavenumber k_β.

The plasma equilibrium is maintained by a background of ions uniform within the annulus and assumed fixed (*i.e.*, infinitely massive). Such an equilibrium is rather idealized, but approximates the situation of interest in a number of applications, the two most prominent being (1) a laser-formed channel,[14] and (2) an electron-beam formed channel in a pre-formed plasma.[13] In the case of the laser-formed channel, the plasma gradient is produced by expansion of the plasma following the laser pulse. For the beam-formed channel, the plasma annulus would result from laser ionization[15] of a column of radius b_2, followed by expulsion of plasma electrons by the electron-beam. In this case, b_1 is the "neutralization radius", *i.e.*, the radius such that the enclosed ion-charge is sufficient to neutralize the beam electrostatic field. Using Gauss's law one can show that $b_1 = 2\nu k_p^{-1}$, where k_p is the plasma wavenumber, $k_p^2 = 4\pi n_p e^2/mc^2$. The electron charge is $-e$, the electron mass is m and c is the speed of light. Here $\nu = I/I_0$ is Budker's parameter[13] with I the beam current and $I_0 \sim mc^3/e \sim 17$kA. Note that neglect of plasma

return currents requires $k_p b_1 << 1$, or $v << 1$, *i.e.*, low current.[16] Throughout this work ion-motion[5] and beam-head erosion[17] will be neglected. Retardation within the beam-pipe is neglected.

The equilibrium plasma electron charge density is assumed to take the form $\rho_{e0} = -e n_e H(b_2 - r) H(r - b_1)$ and the beam charge density is $\rho_{b0} = -e n_b H(a - r)$ where H is the step function, $-e$ is the electron charge, n_b is the equilibirum number density for the beam, and n_e is the initial plasma number density.

We consider the effect of a perturbation to the beam centroid in the form of a small displacement, ξ, in the x-direction, as depicted in Fig. 2. The perturbation to the beam charge density is then $\rho_{b1} = -e n_b \xi \delta(a - r) \cos\theta$ where θ is the azimuth and δ is the Dirac delta function.

Maxwell's equations are most simply expressed in terms of the perturbed vector potential A_z and the "pinch potential" $\psi \equiv A_z - \phi$, with ϕ the perturbed scalar potential. The Lorentz gauge is assumed and the "frozen-field" approximation is enforced, with which the D'Alembertian operator is replaced by the transverse Laplacian $\nabla_\perp^2$ and radiative effects are neglected, corresponding to the limit $k_p R/\gamma << 1$. Maxwell's equations reduce to

$$\nabla_\perp^2 \begin{pmatrix} \psi \\ A_z \end{pmatrix} = -4\pi \begin{pmatrix} -\rho_{e1} \\ \rho_{b1} \end{pmatrix}, \tag{1}$$

The perturbed plasma electron charge density, ρ_{e1}, is determined from the potentials through the electron cold-fluid equations,

$$\frac{\partial \rho_{e1}}{\partial t} + \vec{\nabla}_\perp \bullet \left(\rho_{e0} \vec{V}_e \right) \approx 0, \tag{2}$$

$$\frac{\partial V_e}{\partial t} \approx \frac{e}{m} \vec{\nabla}_\perp \phi, \tag{3}$$

where $\dot{V}_e$ is the plasma-electron velocity, and t is time.

To close this system one needs the Lorentz force law describing the deflection of the beam centroid ξ. This takes the form

$$\left(\frac{\partial}{\partial z} \gamma \frac{\partial}{\partial z} + \gamma k_\beta^2 \right) \xi = - \frac{e}{m c^2} \frac{\partial \psi}{\partial x}, \tag{4}$$

where γ is the Lorentz factor for the beam, c is the speed of light, and the z-derivative is taken with the "beam coordinate" $\tau = t - z/c$ fixed. Henceforth we will use variables z, τ rather than z, t. Thus the beam centroid $\xi = \xi(z, \tau)$ varies along the beam (in τ) and varies along the beamline (in z) due to focusing, acceleration, and electrostatic deflection by the plasma sheath.

We proceed by rewriting the fluid equations as

$$\frac{\partial^2 \rho_{e1}}{\partial \tau^2} + \frac{\rho_{e0} e}{m} \nabla_\perp^2 \phi = - \frac{e}{m} \vec{\nabla} \rho_{e0} \bullet \vec{\nabla}_\perp \phi. \tag{5}$$

In this form it is clear that ρ_{e1} consists of polarization layers located at the discontinuities in ρ_{e0}, i.e., at $r = b_1$ and $r = b_2$. Thus ρ_{e1} may be expressed as

$$\rho_{e1} = e n_e \left\{ \eta_1 \, \delta(r - b_1) - \eta_2 \, \delta(r - b_2) \right\} \cos\theta, \tag{6}$$

where $\eta_1(z,\tau)$ and $\eta_2(z,\tau)$ are dynamic variables representing the displacements of the centroids of the inner and outer surfaces of the plasma annulus. Integrating the fluid equations alternately across each surface, there result two equations for the annulus variables,

$$\left\{\frac{\partial^2}{\partial\tau^2}+\omega_0^2\right\}en_e\eta_j\cos\theta=\frac{\omega_0^2}{2\pi}\overline{\left(\frac{\partial\phi}{\partial r}\right)}_{r=b_j}. \tag{7}$$

here j=1,2 and $\omega_0=\omega_p/2^{1/2}$, with $\omega_p=k_pc$ the plasma frequency. The bar indicates an average of the (discontinuous) derivatives at the surface.

Having determined the beam and annulus response to the fields, in Eqs. (4) and (7), it remains only to determine the fields in terms of ξ, η_1, and η_2. The solution for the vector potential takes the form

$$A_z=\cos(\theta)\begin{cases} Ar & ;\quad 0<r<a \\ Br+Cr^{-1} & ;\quad a<r<R \end{cases}, \tag{8}$$

where the parameters A, B, and C are determined from the conducting boundary condition at $A_z(R)=0$, continuity at $r=a$, and the discontinuity in derivative specified by Eq. (1). The result is

$$A = -2\pi e n_b \xi \left(1 - \frac{a^2}{R^2}\right) \tag{9}$$

$$B = 2\pi e n_b \xi \frac{a^2}{R^2} \tag{10}$$

$$C = -2\pi e n_b \xi a^2 \tag{11}$$

The pinch potential takes the form

$$\psi = \cos(\theta)\begin{cases} Dr & ; \quad 0 < r < b_1 \\ Er + Fr^{-1} & ; \ b_1 < r < b_2 \\ Gr + Hr^{-1} & ; \ b_2 < r < R \end{cases}, \tag{12}$$

where the coefficients *D, E, F, G,* and *H* are determined from continuity in ψ, the discontinuities in derivative specified by Eq. (5), and the conducting boundary condition $\psi(R)$=0. Some lengthy algebra reveals

$$D = -2\pi e n_e \eta_1 \left(1 - \frac{b_1^2}{R^2}\right) + 2\pi e n_e \eta_2 \left(1 - \frac{b_2^2}{R^2}\right), \tag{13}$$

$$E = 2\pi e n_e \eta_1 \frac{b_1^2}{R^2} + 2\pi e n_e \eta_2 \left(1 - \frac{b_2^2}{R^2}\right), \tag{14}$$

$$F = -2\pi e n_e \eta_1 b_1^2, \tag{15}$$

$$G = 2\pi e n_e \eta_1 \frac{b_1^2}{R^2} - 2\pi e n_e \eta_2 \frac{b_2^2}{R^2}, \tag{16}$$

$$H = -2\pi e n_e \eta_1 b_1^2 + 2\pi e n_e \eta_2 b_2^2. \tag{17}$$

With these expressions in hand, it is straightforward to compute ϕ. With some algebra we have

$$\overline{\left(\frac{\partial\phi}{\partial r}\right)}_{r=b_1} = \left\{B - C\,b_1^{-2} - \frac{1}{2}\left(E + D - F\,b_1^{-2}\right)\right\}\cos\theta$$
$$= 2\pi e n_b a^2 \xi\left(\frac{1}{R^2} + \frac{1}{b_1^2}\right)\cos\theta - 2\pi e n_e\left(\eta_1\frac{b_1^2}{R^2} + \eta_2\left(1 - \frac{b_2^2}{R^2}\right)\right)\cos\theta, \tag{18}$$

$$\overline{\left(\frac{\partial\phi}{\partial r}\right)}_{r=b_2} = \left\{B - C\,b_2^{-2} - \frac{1}{2}\left(E + G - F\,b_2^{-2} - H\,b_2^{-2}\right)\right\}\cos\theta$$
$$= 2\pi e n_b a^2 \xi\left(\frac{1}{R^2} + \frac{1}{b_2^2}\right)\cos\theta - 2\pi e n_e\left(\eta_1\left(\frac{b_1^2}{R^2} + \frac{b_1^2}{b_2^2}\right) - \eta_2\frac{b_2^2}{R^2}\right)\cos\theta. \tag{19}$$

Substituting these coefficients in Eq. (7) the result is

$$\left\{\frac{\partial^2}{\partial\tau^2} + \omega_1^2\right\} e n_e \eta_1 = \omega_0^2 e n_b \xi\left(\frac{a^2}{b_1^2} + \frac{a^2}{R^2}\right) - \omega_0^2 e n_e \eta_2\left(1 - \frac{b_2^2}{R^2}\right), \tag{20}$$

$$\left\{\frac{\partial^2}{\partial\tau^2} + \omega_2^2\right\} e n_e \eta_2 = \omega_0^2 e n_b \xi\left(\frac{a^2}{b_2^2} + \frac{a^2}{R^2}\right) - \omega_0^2 e n_e \eta_1\left(\frac{b_1^2}{R^2} + \frac{b_1^2}{b_2^2}\right), \tag{21}$$

where we abbreviate

$$\omega_1^2 = \omega_0^2\left(1 + \frac{b_1^2}{R^2}\right), \tag{22}$$

$$\omega_2^2 = \omega_0^2 \left(1 - \frac{b_2^2}{R^2}\right). \tag{23}$$

Note that $\omega_2^2 \le \omega_0^2 \le \omega_1^2$. For subsequent analysis, Eqs. (22) and (23) are most simply written as

$$\left\{\frac{\partial^2}{\partial \tau^2} + \omega_1^2\right\}\eta_1 = \mu_1^2 \xi - \nu_1^2 \eta_2, \tag{24}$$

$$\left\{\frac{\partial^2}{\partial \tau^2} + \omega_2^2\right\}\eta_2 = \mu_2^2 \xi - \nu_2^2 \eta_1, \tag{25}$$

where the coefficients are

$$\mu_j^2 = \frac{1}{2}\omega_b^2 \frac{a^2}{b_j^2}\left(1 + \frac{b_j^2}{R^2}\right), \tag{26}$$

$$\nu_1^2 = \omega_0^2 \left(1 - \frac{b_2^2}{R^2}\right), \tag{27}$$

$$\nu_2^2 = \omega_0^2 \left(\frac{b_1^2}{R^2} + \frac{b_1^2}{b_2^2}\right), \tag{28}$$

with $\omega_b{}^2 = 4\pi n_b e^2/m$.

These equations are coupled to that for the beam

$$\left\{\frac{\partial}{\partial z}\gamma \frac{\partial}{\partial z} + \gamma k_\beta^2\right\}\xi = \kappa_1^2 \eta_1 - \kappa_2^2 \eta_2, \tag{29}$$

where the constants

$$\kappa_j^2 = \frac{\omega_0^2}{c^2}\left(1 - \frac{b_j^2}{R^2}\right), \tag{30}$$

Equations (24), (25) and (29) provide a complete description of the linear evolution of the electron-hose instability in an annular sheath geometry, in the large skin-depth limit.

III. WAKEFIELD FORMULATION

To understand the behavior of this system, consider first the homogeneous problem with ξ=0, corresponding to a freely vibrating sheath. For a perturbation varying as $\eta_1, \eta_2 \propto exp(-i\omega\tau)$, Eqs.(24) and (25) take the form

$$\begin{pmatrix} \omega_1^2 - \omega^2 & \nu_1^2 \\ \nu_2^2 & \omega_2^2 - \omega^2 \end{pmatrix}\begin{pmatrix} \eta_1 \\ \eta_2 \end{pmatrix} = 0. \tag{31}$$

A non-trivial solution results only if the determinant of the matrix vanishes, and this condition is the eigenvalue equation for the angular frequency ω,

$$\left(\omega^2 - \omega_2^2\right)\left(\omega^2 - \omega_1^2\right) = \nu_1^2\nu_2^2. \tag{32}$$

The solutions for the eigenfrequencies take the form

$$\omega_{\pm}^2 = \frac{\omega_1^2 + \omega_2^2}{2} \pm \sqrt{\left(\frac{\omega_1^2 - \omega_2^2}{2}\right)^2 + \nu_1^2 \nu_2^2}$$
$$= \omega_0^2 \left\{ 1 - \frac{b_2^2 - b_1^2}{2R^2} \pm \sqrt{\left(\frac{b_2^2 - b_1^2}{2R^2}\right)^2 + \frac{b_1^2}{b_2^2}} \right\}, \tag{33}$$

corresponding to symmmetric (ω_-) and antisymmetric (ω_+) modes of coupled vibration. The roots are always real as one would expect for a cold, collisionless plasma. From Eq. (33) one can also show that $\omega_-^2 \le \omega_0^2 \le \omega_+^2 \le \omega_p^2$.

Next we solve for the response of the system to a sharp impulse, $\xi=\delta(\tau)$. For $\tau>0$, the solution must be a superposition of the eigenmodes of the homogeneous system, with displacements vanishing at $\tau=0$. Thus

$$\eta_j = \eta_j^+ \sin(\omega_+ \tau) + \eta_j^- \sin(\omega_- \tau), \tag{34}$$

where, from Eq. (31), the eigenmode amplitudes must be related according to

$$\eta_1^{\pm} = \frac{\nu_1^2}{\omega_{\pm}} \rho_{\pm} \sin(\omega_{\pm} \tau), \tag{35}$$

$$\eta_2^{\pm} = \frac{\left(\omega_{\pm}^2 - \omega_1^2\right)}{\omega_{\pm}} \rho_{\pm} \sin(\omega_{\pm} \tau), \tag{36}$$

with constants $\rho_{\pm}$ determined by the initial excitation. From Eqs. (24) and (25),

$$\frac{\partial \eta_j}{\partial \tau}\left(0^+\right) = \int_{0^-}^{0^+} \mu_j^2 \xi = \mu_j^2, \tag{37}$$

and in terms of $\rho_{\pm}$ this is

$$\begin{pmatrix} 1 & 1 \\ \omega_+^2 - \omega_1^2 & \omega_-^2 - \omega_1^2 \end{pmatrix} \begin{pmatrix} \rho_+ \\ \rho_- \end{pmatrix} = \begin{pmatrix} \mu_1^2 / \nu_1^2 \\ \mu_2^2 \end{pmatrix}, \tag{38}$$

with the solution,

$$\rho_{\pm} = \pm \frac{\left(\omega_1^2 - \omega_m^2\right)\mu_1^2 + \mu_2^2 \nu_1^2}{\nu_1^2 \left(\omega_+^2 - \omega_-^2\right)}. \tag{39}$$

For a more general beam impulse, the result for the sheath displacements may be obtained from superpostion,

$$\begin{pmatrix} \eta_1 \\ \eta_2 \end{pmatrix}(z,\tau) = \int_0^{\tau} d\tau' \left\{ \sum_{\pm} \begin{pmatrix} \nu_1^2 \\ \omega_{\pm}^2 - \omega_1^2 \end{pmatrix} \rho_{\pm} \frac{\sin\left[\omega_{\pm}\left(\tau - \tau'\right)\right]}{\omega_{\pm}} \right\} \xi(z,\tau'). \tag{40}$$

Substituting this result in Eq. (29), we arrive at an equation for the evolution of the beam centroid, in a form familiar in studies of beam break-up,[18]

$$\left\{ \frac{\partial}{\partial z} \gamma \frac{\partial}{\partial z} + \gamma k_\beta^2 \right\} \xi(z,\tau) = \int_0^{\tau} d\tau' \, G\left(\tau - \tau'\right) \xi(z,\tau'), \tag{41}$$

where the Green's function G is just a sum of the wakefields excited in each mode,

$$G(\tau) = \sum_{\pm} G_{\pm} \sin(\omega_{\pm}\tau), \tag{42}$$

and

$$\begin{aligned} G_{\pm} &= \frac{\rho_{\pm}}{\omega_{\pm}}\left\{\kappa_2^2\left(\omega_1^2 - \omega_{\pm}^2\right) + \nu_1^2\kappa_1^2\right\} \\ &= \frac{\rho_{\pm}}{\omega_{\pm}}\frac{\omega_0^2}{c^2}\left(1 - \frac{b_2^2}{R^2}\right)\left(\omega_p^2 - \omega_{\pm}^2\right). \end{aligned} \tag{43}$$

More explicitly this can be written as,

$$G_{\pm} \pm 2\nu\left(\frac{1}{b_1^2} + \frac{1}{R^2}\right)\frac{\left(\omega_p^2 - \omega_{\pm}^2\right)\left(\omega_o^2\chi - \omega_{\mathrm{m}}^2\right)}{\omega_{\pm}\left(\omega_{+}^2 - \omega_{-}^2\right)}, \tag{44}$$

where

$$\chi = 1 + \frac{b_1^2}{R^2} + \frac{b_1^2}{b_2^2}\left(1 - \frac{b_2^4}{R^4}\right)\left(1 + \frac{b_1^2}{R^2}\right)^{-1}. \tag{45}$$

It will be helpful to have the slope of the wakefield for small τ,

$$G' = \sum_{\pm} \omega_{\pm} G_{\pm} = 2\nu\omega_0^2\left(\frac{1}{b_1^2} - \frac{1}{b_2^2}\right)\left(1 + \frac{b_1^2 b_2^2}{R^4}\right). \tag{46}$$

These results simplify considerably in either of the limits $R \to \infty$

$$\lim_{R\to\infty} G_{\pm} = \frac{I}{I_0}\frac{\omega_0^2}{\omega_{\pm} b_1^2}\left(1 - \frac{b_1^2}{b_2^2}\right), \tag{47}$$

$$\lim_{R\to\infty} \frac{\omega_{\pm}^2}{\omega_0^2} = 1 \pm \frac{b_1}{b_2}, \tag{48}$$

or $b_2 \to R$, where $G_- \to 0, \omega_- \to 0$, and

$$\lim_{b_2\to R} G_{+} = 2\nu\frac{\omega_0^2}{\omega_{+}}\frac{1}{b_1^2}\left(1 - \frac{b_1^4}{R^4}\right), \tag{49}$$

$$\lim_{b_2\to R} \frac{\omega_{+}^2}{\omega_0^2} = 1 + \frac{b_1^2}{R^2}. \tag{50}$$

IV. SINGLE-BUNCH BEAM BREAK-UP

To calculate the asymptotic growth we will specialize to the case of a bunch much shorter than the natural periods of the wakefield ("single-bunch beam breakup"). In the limit of a short pulse, the wake is approximately linear, $G(\tau) \approx G'\tau$. For illustration, examples will assume the ion-focusing condition, $\gamma k_\beta{}^2 \tilde{} k_0{}^2$ with $k_0{}^2 = k_p{}^2/2$, corresponding to the case where the channel is filled with unneutralized ions equal in density to that in the surrounding sheath.

First we consider the case of no acceleration ("coasting beam"). The asymptotic form for the beam centroid in this case is well-known,[1]

$$\xi(z,\tau) \approx \frac{3^{1/4}}{2^{3/2}\pi^{1/2}} A_1^{-1/2} e^{A_1} \cos\left\{ k_\beta z - 3^{-1/2} A_1 + \frac{\pi}{12} \right\},$$

(51)

where the exponent $A_1=(z/L_1)^{1/3}$, with growth length,

$$L_1 = \frac{2^6}{3^{9/2}} \frac{\gamma k_\beta}{G'\tau^2}.$$

(52)

This result assumes strong focusing $L>\lambda_\beta$, and this condition imposes an upper bound on the product of charge and bunch length, since the length scale varies as $(Q\tau)^{-1}$. Eq. (52) can be cast in a more transparent form assuming ion-focusing,

$$L_1 \approx 3.6 \times 10^{-2} \lambda_\beta \left(\omega_p \tau\right)^{-2} \Lambda^{-2} \nu^{-1},$$

(53)

where

$$\Lambda^2 = \left(\frac{1}{\left(k_p b_1\right)^2} - \frac{1}{\left(k_p b_2\right)^2} \right) \left(1 + \frac{b_1^2 b_2^2}{R^4} \right).$$

(54)

For illustration, consider a bunch of charge Q~100pC travelling through a plasma channel with n_p=1x10^{17}cm^{-3}, corresponding to λ_p=100μm. We take $R\rightarrow\infty$ and b_1/b_2=0.5, with $k_p b_1$=1 or b_1=16μm so that Λ~0.87. We assume a bunch length $\omega_p\tau=2\pi/100$ or τ~3 fs. The peak current I~Q/τ~30kA corresponding to Budker parameter ν~1.8.

This gives $L_1 \tilde{} 22\lambda_\beta$. For a beam energy of 10MeV ($\gamma_i \tilde{} 20$) the betatron period $\lambda_\beta = (2\gamma)^{1/2}\lambda_p$ is 630μm and the propagation range to 100-fold growth in the beam centroid ($A_1 \tilde{} 6.9$) is about 5m. This is a rather short range and it suggests that one consider injection at a higher energy, and take into account the salubrious effect of acceleration.

To determine the asymptotic growth with acceleration, we apply an eikonal approximation to Eq. (41), assuming that growth will turn out to be slow on the scale of a betatron period. We define a slowly varying amplitude χ, in terms of which ξ may be expressed as

$$\xi(z,\tau) = \Re\left\{\left(\frac{\gamma(0)k_\beta(0)}{\gamma(z)k_\beta(z)}\right)^{1/2}\chi(z,\tau)\exp\left(i\theta_\beta(z)\right)\right\}, \tag{55}$$

with the betatron phase,

$$\theta_\beta(z) = \int_0^z dz k_\beta = \frac{2k_0}{g}\left(\gamma(z)^{1/2} - \gamma(0)^{1/2}\right), \tag{56}$$

and we take $\gamma k_\beta{}^2 \tilde{} k_0{}^2 = k_p{}^2/2$) and $\gamma = \gamma_0 + gz$. Substituting Eq. (55) in Eq. (41), and performing a Laplace transform in τ, one can show that

$$\frac{\partial\tilde{\chi}}{\partial z}(z,p) = \frac{\tilde{G}(p)}{2i\gamma k_\beta}\tilde{\chi}(z,p), \tag{57}$$

where the tilde denotes the Laplace transform, and p is the Laplace transform variable. Inverting the Laplace transform, the solution for the beam centroid is

$$\chi(z,\tau) = \frac{1}{2\pi i}\int_{-i\infty}^{i\infty} dp\, \frac{1}{p} \exp\left\{ p\tau - i\frac{G'}{gk_0 p^2}\left(\gamma(z)^{1/2} - \gamma(0)^{1/2}\right)\right\}, \tag{58}$$

and we have used $\tilde{G}(p) = G'/p^2$. This integral may be computed approximately by the method of steepest descents,[19] and the result for the beam centroid displacement is

$$\xi(z,\tau) \approx \frac{3^{1/4}}{2^{3/2}\pi^{1/2}}\left(\frac{\gamma(0)}{\gamma(z)}\right)^{1/4} \frac{e^{A_2}}{A_2^{1/2}} \cos\left\{\theta_\beta - 3^{-1/2}A_2 + \frac{\pi}{12}\right\}, \tag{59}$$

with exponent

$$A_2 = \frac{3^{3/2}}{2^{5/3}}\left\{\frac{G'\tau^2}{gk_0}\left(\gamma(z)^{1/2} - \gamma(0)^{1/2}\right)\right\}^{1/3}. \tag{60}$$

Asymptotically, $A_2 \to (z/L_2)^{1/6}$, with

$$L_2 \approx 2.6\times 10^{-2}\left(gk_p^{-2}\right)\left[\left(\omega_p\tau\right)^{-2}\Lambda^{-2}\nu^{-1}\right]^2. \tag{61}$$

Comparing this with Eq. (53), one sees that the length scale λ_β has been replaced with the length scale gk_p^{-2}, and varies as $(Q\tau)^{-2}$, a much more favorable scaling.

For illustration we consider a numerical example corresponding to a 2.5 TeV accelerator. As in the previous example, we assume

Q~100pC, n_p=1x10^{17}cm^{-3}, λ_p=100μm, τ~3 fs, I~30kA, v~1.8, $R\rightarrow\infty$, b_1/b_2=0.5, and b_1=16μm. However, in this case, we assume injection at a *high* energy, 10GeV (γ_i~2x10^4) followed by acceleration to 2.51TeV (γ_f~5x10^6). The betatron period $\lambda_\beta=(2\gamma)^{1/2}\lambda_p$ is initially 2cm and increases to 30cm at the exit. With these parameters fixed, we consider three cases corresponding to different accelerating gradients: (1) 1 GeV/m (2) 10GeV/m and (3) 100GeV/m. Associated parameters are listed in Table 1. To check these scalings we solve Eq. (41) numerically with results indicated in Fig. 3. The analytic results are the dashed curves overlayed in Fig. 3 and they are almost indistinguishable from the numerical results. Evidently only in the lower gradient case is the instability cause for concern.

V. CONCLUSIONS

Transverse two-stream instability in an annular plasma geometry has been analyzed in the limit of low plasma return current. Asymptotic growth for an accelerated beam has been computed for several illustrative examples and compared to more exact numerical results giving good agreement. While the coasting beam scalings appear quite severe at low energy, single-bunch instability growth can in fact be reduced to nil, for a very high-gradient accelerator.

ACKNOWLEDGMENTS

This work has benefited from discussions with Jonathan Krall and collaboration on related topics with Martin Lampe and Glenn Joyce. Work was supported by U.S. Dept. of Energy contract AC03-76SF-00515.

REFERENCES

[1] Y. Y. Lau, Phys. Rev. Lett. **63**, 1141 (1989).

[2] V. K. Neil, L. S. Hall and R. K. Cooper, Part. Accel. **9**, 213 (1979).

[3] S. Bodner, V. K. Neil, and L. Smith, Particle Accelerators **1**, 327 (1970).

[4] R. J. Adler, B. B. Godfrey, M. M. Campbell, D. J. Sullivan, and T. C. Genoni, Particle Accelerators **13**, 25 (1983).

[5] H. L. Buchanan, Phys. Fluids **30**, 221 (1987).

[6] E. P. Lee, Phys. Fluids **21**, 1327 (1978); M. Lampe, W. Sharp, R. F. Hubbard, E. P. Lee, and R. J. Briggs, Phys. Fluids **27**, 2921 (1984).

[7] D. R. Welch and T. P. Hughes Phys. Fluids **B** 5, 339 (1993).

[8] M. Lampe, G. Joyce, S. P. Slinker, and D. H. Whittum, Phys. Fluids. **B** 5, 1888 (1993).

[9] T.W.L. Sanford, Phys. Plasmas **2**, 2539 (1995).

[10] S. Riyopoulos, D. Chernin, and D. Dialetis, Phys. Plasmas **2**, 3194 (1995).

[11] P.W. Werner, E. Schamiloglu, J.R. Smith, K. W. Struve, and R. J. Lipinski, Phys. Rev. Lett. **73,** 2986 (1994).

[12] T.C. Chiou, T. Katsouleas, C. Decker, W.B. Mori, J.S. Wurtele, G. Shvets, J.J. Su, Phys. Plasmas **2**, 310 (1995).

[13] J. Rosenzweig, B. Breizman, T. Katsouleas, and J.J. Su, Phys. Rev. A **44**, 6189 (1991).

[14] C.G. Durfee III and H.M. Milchberg, Phys. Rev. Lett. **71**, 2409 (1993).

[15] C. A. Frost, J. R. Woodworth, J. N. Olsen And T. A. Green, Appl. Phys. Lett. **41**, 813 (1982).

[16] D. H. Whittum, Phys. Fluids B **4**, 476 (1992).

[17]J. Krall, K. Nguyen, and G. Joyce, Phys. Fluids B **1**, 2099 (1989).

[18] K. L. F. Bane, *Physics of Particle Accelerators,* AIP Conf. Proc. **153**, edited by Melvin Month and Margaret Dienes (AIP, New York, 1987), pp. 972-1012.

[19] D. H. Whittum, M. Lampe, G. Joyce, S.P. Slinker, S.S. Yu, and W.M. Sharp, Phys. Rev. A **46**, 6684 (1992).

Table 1. Parameters for three 2.5 TeV accelerator examples.

Gradient	1GeV/m	10GeV/m	100GeV/m
Length, z	2500m	250m	25m
Betatron Periods	16000	1600	160
$g = d\gamma/dz$	$10^3 m^{-1}$	$10^4 m^{-1}$	$10^5 m^{-1}$
Exponent A_2	12.9	6.0	2.8
Analytic ξ	7.4×10^3	11	0.6
Numeric ξ	7.6×10^3	10	0.6

FIG. 1. In equilibrium, a relativistic electron beam of radius a propagates in the z-direction (out of the page). Plasma electrons and ions fill an annulus of inner radius b_1 and outer radius b_2. The inner channel could be neutral or consist of unneutralized ions.

FIG. 2. A displacement of the beam centroid by an amount ξ in the x-direction, induces a displacement η_1 of the inner surface of the plama, and a displacment η_2 of the outer surface. The resulting polarization of the channel deflects follow-on portions of the beam, resulting in instability.

FIG. 3. Depicted is evolution of the amplitude of the beam centroid oscillation $|\xi|$ through 2.5TeV of acceleration as computed numerically from Eq. (41). The amplitude is evaluated at the pulse tail for three different accelerating gradients: 1GeV/m, 10GeV/m and 100GeV/m. Dashed curves are the analytic amplitudes from Eq. (59).

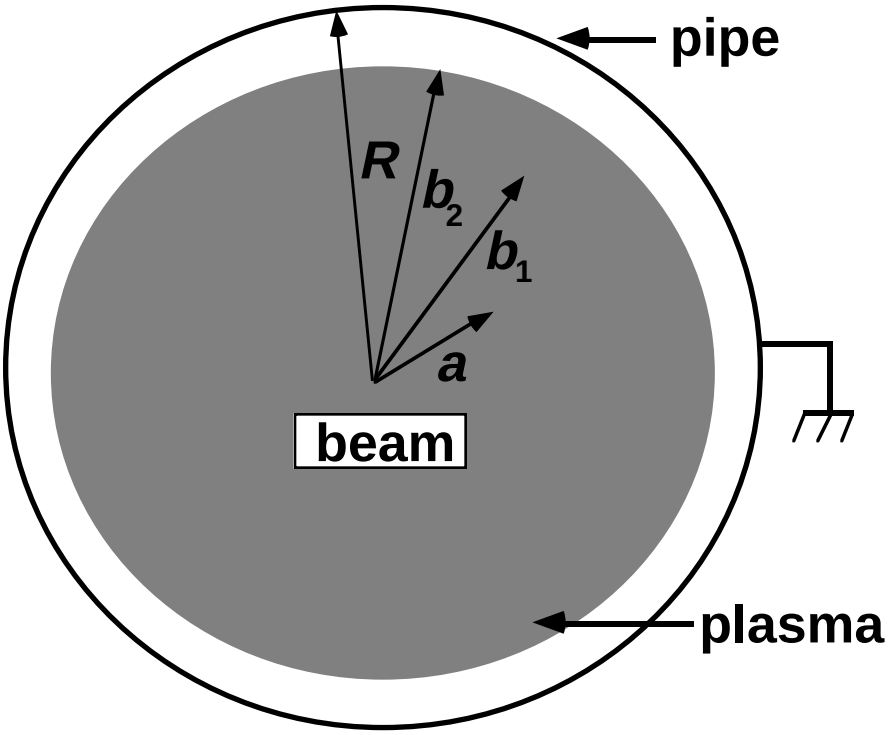

FIG. 1

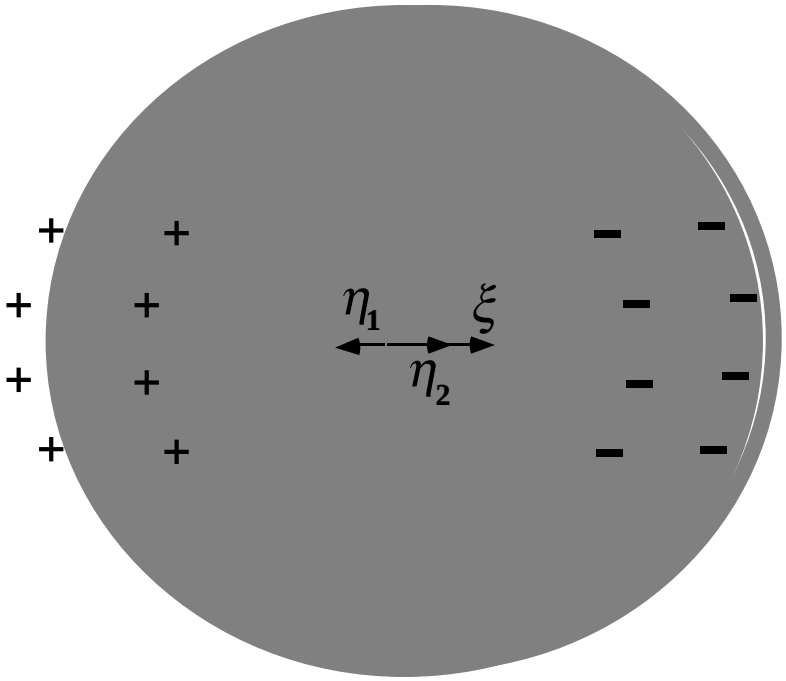

FIG. 2

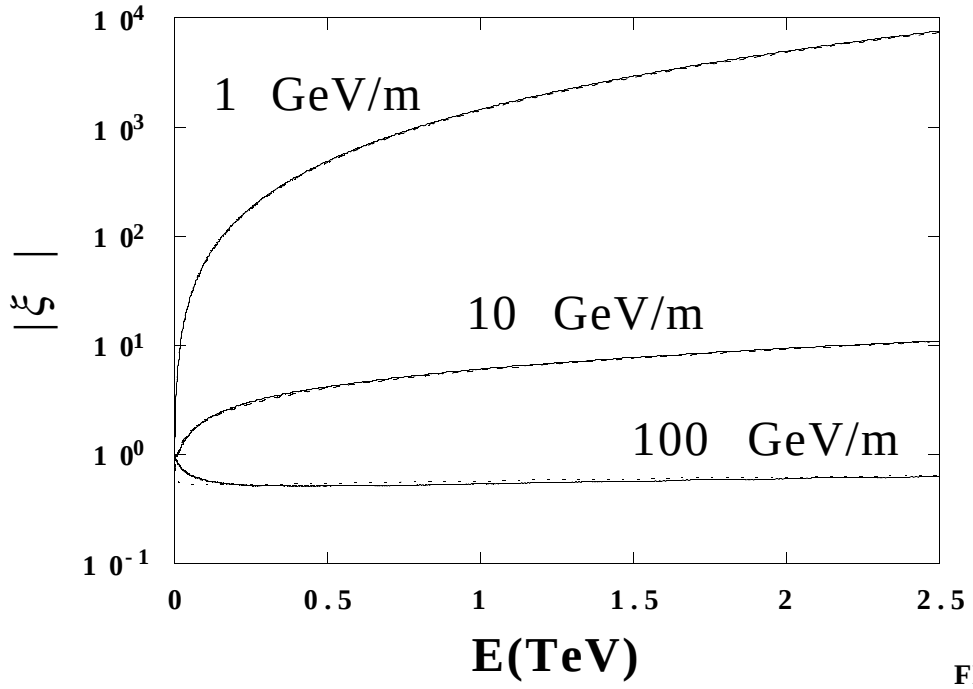
1 0^4
1 0^3
1 0^2
1 0^1
1 0^0
1 0^-1
ξ
1 GeV/m
10 GeV/m
100 GeV/m
0
0.5
1
1.5
2
2.5
E(TeV)

FIG. 3